Optical Constants of Sulfuric Acid; Application to the Clouds of Venus?

Kent F. Palmer and Dudley Williams

With the purpose of obtaining the real and imaginary parts of the complex refractive index $\hat{N} = n + ik$, we have made quantitative measurements of spectral transmission and reflection of sulfuric acid solutions in the visible and near infrared. On the basis of the results, we have obtained values for n throughout the entire region and values of k in the near infrared together with upper limits for k in the visible region. These optical constants can be used to interpret the results of polarization studies of solar radiation that has been scattered by the clouds of Venus. We have Kramers-Kronig phase-shift analysis to obtain values of n and k from reflection measurements in the intermediate infrared region (400–4000 cm^{-1}). Our measurements were made at 300 K on sulfuric acid solutions having concentrations by weight of 95.6, 84.5, 75, 50, 38, and 25%. If the particles in the Venus clouds consist of liquid droplets of sulfuric acid at a temperature of 250 K, comparison of existing Venus data with our data suggests that the acid concentration is probably higher than 70%. Various possibilities are discussed.

Introduction

From balloon soundings, Rosen[1] has found that sulfuric acid particles are the most abundant aerosols in the earth's stratosphere. The sizes and shapes of these particles as well as the phases of the $H_2SO_4 \cdot nH_2O$ involved have not yet been definitely established. In order to provide laboratory data for comparison with aerosol spectra in the 800–1250 cm^{-1} atmospheric window, Remsberg[2] has used ATR techniques to obtain values of the complex index of refraction $\hat{N} = n + ik$ in this spectral region. Because of strong sulfuric acid bands in this atmospheric window, Neumann[3] has pointed out that variations in the abundance of H_2SO_4 aerosols in the stratosphere could have an influence on climatic conditions.

On the basis of polarization studies of scattered radiation in the visible region, along with estimates of pressure, temperature, and relative humidity based on infrared studies of the planet, Young[4] and Sill[5] have independently suggested that the clouds of Venus may well consist of $H_2SO_4 \cdot nH_2O$ particles. More recently, Hansen and Hovenier[6] have shown that measured values of the polarization of solar radiation scattered by the Venus clouds can be accounted for on the basis of spherical particles with a size distribution sharply peaked at a radius of approximately 1 μm with the following values of refractive index n: 1.46 at 365 nm, 1.44 at 550 nm, and 1.43 at 990 nm. The acceptable limit of uncertainty δn is ± 0.015 at each of these wavelengths. The temperature[4] at the top of the main cloud bank is approximately 250 K; the optical thickness of the cloud cover is unity in a region where the pressure is 50 mbars.[6]

In order to obtain more detailed information from existing and future observational data, it is desirable to obtain laboratory measurements of n and k for sulfuric acid solutions in the entire spectral region from the ultraviolet to the remote infrared. In the present study, we have attempted to supply the needed laboratory data for a wide range of sulfuric acid concentrations. All our work has been done at 300 K; Lorentz-Lorenz corrections can be applied to obtain values of n and k for liquid samples at other temperatures. We have not yet attempted to determine optical constants for the crystal hydrates of sulfuric acid; work on the solid hydrates involves formidable experimental difficulties.

The general experimental techniques employed are similar to those used in our earlier studies of water.[7–12] They involve quantitative measurements of reflectance at near-normal incidence and measurements of the transmittance of samples in carefully constructed cells of known thickness. Kramers-Kronig phase-shift analysis of the reflectance data gives values of n with a fractional uncertainty $\delta n/n = \pm 0.01$ over most of the spectral range of measurement and corresponding values of k having an uncertainty $\delta k = \pm 0.03$ in most regions.

The authors are with the Physics Department, Kansas State University, Manhattan, Kansas 66506.
Received 12 July 1974.

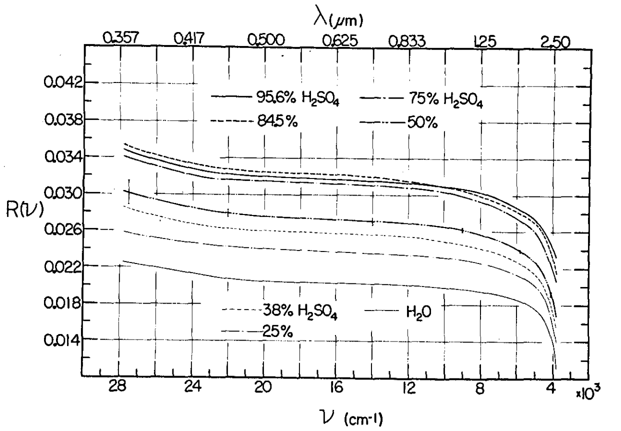

Fig. 1. Spectral reflectance of H_2SO_4 solutions in the 4000–28,000 cm^{-1} region.

Results in the Visible and Near Infrared

In the visible and near infrared, we used the combination of reflection and transmission measurements described in our earlier paper.[12] In the reflection measurements, we first compared the radiant flux reflected from the free surface of an acid sample with the flux reflected from a reference mirror, the absolute reflectance of which had been measured by means of a Strong reflectometer. From these measurements, the near-normal fractional spectral reflectance R of the acid sample can be obtained with fractional uncertainty $\delta R/R$ of approximately ± 0.02.

Because of hygroscopic properties of sulfuric acid, the concentration of the free surface layer of a sulfuric acid sample changes when the sample is exposed to air. We were careful to use freshly prepared solutions in each set of reflection measurements and to reject data sets in which reflectance had measurably changed in the course of a series of separate runs.

The spectral reflectances R for 95.6, 84.5, 75, 50, 38, and 25% H_2SO_4 solutions are summarized in Fig. 1 for the spectral range 4800–28000 cm^{-1}; the uncertainties δR in various spectral regions given on the curve for the 50% solution are typical of those for the other solutions. In most of the visible region, spectral reflectance increases monotonically with increasing concentration, except for the 84.5% solution for which the spectral reflectance curve crosses that of the 95.6% solution. The spectral reflectance curves for all solutions fall rapidly at frequencies below 6000 cm^{-1} because of the proximity of strong absorption bands associated with molecules containing OH groups; these strong fundamental bands appear in the 3600–3000 cm^{-1} region.

Although the absorption index k is very small throughout the visible and near infrared, the radiant flux from the sun is large in these spectral regions. Hence, it is possible that absorption of insolation associated with weak bands in these regions could have an influence on planetary heat balances. Therefore, we have made quantitative measurements of the Lambert absorption coefficient α throughout the near infrared region and have established upper limits of α in the visible region.

At a given frequency, the spectral transmittance $T = I/I_0$ giving the ratio flux I transmitted by a liquid-filled absorption cell to the incident flux I_0 is given by the expression

$$T = (1 - A')(1 - R') \exp(-\alpha x), \tag{1}$$

where A' is the spectral absorptance of the cell windows, R' is the reflectance at the outer and inner surfaces of the cell windows, α is the Lambert coefficient, x is the thickness of the absorbing layer of liquid. Accurate determination of A' and R' presents formidable experimental difficulties that can happily be avoided by the use of cells equipped with identical windows but with different thicknesses. By taking ratios of the transmittances of cells of different thickness, it is possible to determine α without actual measurement of A' and R'.

In the present study we used a set of eight precision cells of Infrasil quartz ranging in length x from 1 mm to 5 cm, fabricated from a single batch of Infrasil. At lower frequencies in the near infrared we used a Beckman variable-pathlength cell equipped with quartz windows. This cell provided path lengths x in the range 1 mm to 30 μm. Although the Beckman cell is fabricated from stainless steel and is equipped with a Teflon lining, we were unable to use it in studies of the 50, 38, and 25% solutions, all of which are highly corrosive. Collimated beams were employed in measuring spectral transmittance throughout the region.

Values obtained for the Lambert coefficient α in the 4000–14000 cm^{-1} region are shown graphically for the less-concentrated solutions in Fig. 2, and for the higher concentrations in Fig. 3, along with corresponding curves for water. Because α changes by several orders of magnitude, we give separate linearly expanded plots of α in various spectral intervals in

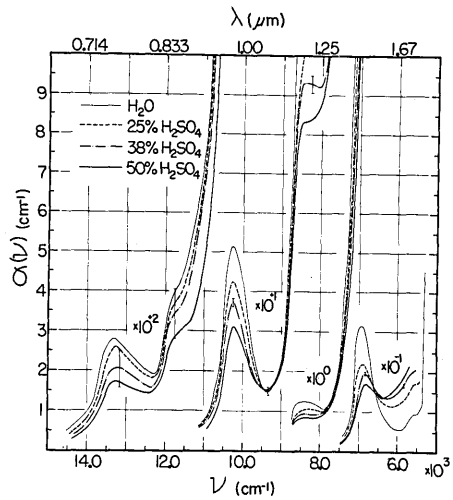

Fig. 2. Lambert absorption coefficients of H_2SO_4 solutions in the 5500–14,500 cm^{-1} region.

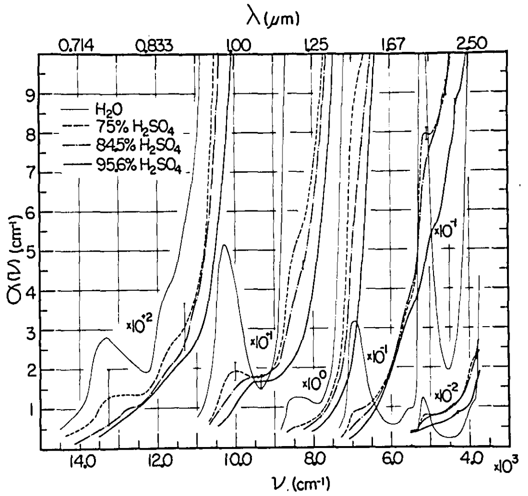

Fig. 3. Lambert absorption coefficients of H_2SO_4 solutions in the 3800–14,500 cm^{-1} region.

these figures along with error bars that indicate uncertainties in the values plotted. Throughout nearly all of the spectral region values of α for the solutions are smaller than the corresponding α value for water. However, near 4200, 5400, and 9600 cm^{-1} in Fig. 3, the α curves for the concentrated solutions are above that of water. The first two of these regions of strong absorption correspond to band positions 4170 and 5460 cm^{-1} reported in the early study of Plyler and Barr.[13] The third region of strong absorption corresponds to a weaker absorption band centered at 9620 cm^{-1} not reported in the earlier study. It is interesting to note that the frequency of the third band is nearly equal to the sum of the frequencies of the other two bands.

Because of limitations imposed by the available absorption cells, we could not obtain α values for frequencies above 14,000 cm^{-1}. In most of the visible region, α values are so small that elaborate experimental arrangements providing for extremely long pathlengths and elimination of scattering would be required for accurate determinations. Because the values of α in the 14,000–28,000 cm^{-1} range are so small as to be of minimal importance to planetary physics, we did not attempt measurements in the present study.

Once α has been determined at a given frequency, values of k can be computed from the defining relation $k = \lambda\alpha/4\pi = \alpha/4\pi\nu$, with ν expressed in cm^{-1}. In the frequency range between 4000 and 14,000 cm^{-1}, k changes by five orders of magnitude.

In terms of n and k, reflectance R at normal incidence is given by the Fresnel relation

$$R = [(n - 1)^2 + k^2]/[(n + 1)^2 + k^2]. \quad (2)$$

The refractive index n can thus be computed from measured values of R and k; throughout the 4000–28,000 cm^{-1} region, k^2 is negligibly small as compared with $(n - 1)^2$. A plot of n as a function of wavenumber for each of the solutions studied is shown in Fig. 4 where the order of the n curves is the same as that of the reflectance curves in Fig. 1. Throughout most of the visible region, the separation of the n curves for the higher concentrations is very small and the limits of uncertainty $\delta n = \pm 0.01n$ overlap. However, the order of the curves in the figure is definitely established by direct comparisons of relative reflectance.

Our results for n and k between the near infrared and near ultraviolet are summarized in Table I, which lists values of the optical constants at selected frequencies for the solutions studied. The frequencies are selected in such a way that values of n and k for other frequencies can be readily interpolated on the basis of the curves shown in Figs. 2–4. All values of n are given to four figures in Table I; however, we point out that the number of actually significant figures varies with frequency and can be estimated from the curves shown in Fig. 4. Similarly, we list k to three figures; the actual uncertainties at various frequencies can be estimated from the error bars shown in Figs. 2 and 3.

Results in the Intermediate Infrared

In contrast to the visible and near infrared, the intermediate infrared region 4000–400 cm^{-1} is a region of such intense absorption that we found it impossible to prepare sufficiently thin, uniform layers of sulfuric acid to obtain values of α from Eq. (1). Because of the corrosive nature of sulfuric acid, we could not employ Robertson's wedge-cell techniques.[9] Instead, we used reflection techniques[7,8] to determine near-normal reflectance and then employed Kramers-Kronig phase-shift analysis to obtain values of n and k.

Although the reflection measurements were essentially similar to those used in earlier studies, we found it convenient in the 2800–1000 cm^{-1} region to use water instead of a reference mirror in studies of the less-concentrated H_2SO_4 solutions. The optical constants of water are sufficiently well known in this spectral region to justify this procedure. Over most

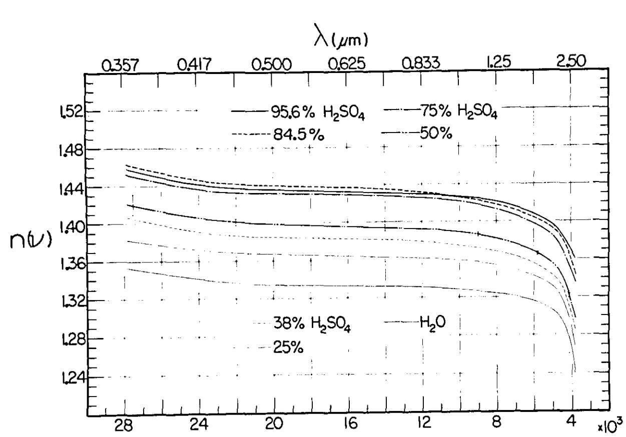

Fig. 4. Refractive indices of H_2SO_4 solutions in the 4000–28,000 cm^{-1} region.

Table I. Optical Constants of Sulfuric Acid from Near Infrared to Ultraviolet

ν	25%		38%		50%		75%		84.5%		95.6%		λ
cm^{-1}	n	k	n	k	n	k	n	k	n	k	n	k	μm
4000	1.286		1.300		1.311		1.344	3.76×10^{-3}	1.358	3.38×10^{-3}	1.368	2.11×10^{-3}	2.500
4100	1.296		1.309		1.321		1.352	2.97	1.363	2.79	1.372	1.86	2.439
4200	1.304		1.316		1.328		1.358	2.41	1.368	2.43	1.376	1.71	2.381
4300	1.310		1.321		1.333		1.362	2.09	1.374	2.13	1.379	1.62	2.326
4400	1.315		1.326		1.338		1.367	1.86	1.378	1.94	1.383	1.41	2.273
4500	1.319		1.330		1.342		1.370	1.67	1.382	1.69	1.385	1.29	2.222
4600	1.323		1.333		1.346		1.374	1.54	1.384	1.56	1.388	1.15	2.174
4700	1.326		1.336		1.348		1.377	1.43	1.388	1.44	1.391	1.02	2.128
4800	1.328		1.339		1.351		1.380	1.35	1.390	1.34	1.393	9.47×10^{-4}	2.083
4900	1.329		1.341		1.353		1.382	1.30	1.392	1.28	1.394	8.93	2.041
5000	1.331		1.343		1.355		1.384	1.26	1.392	1.19	1.396	8.37	2.000
5100	1.332		1.345		1.357		1.386	1.24	1.394	1.10	1.398	7.41	1.961
5200	1.334		1.346		1.358		1.388	1.11	1.396	9.61×10^{-4}	1.399	6.58	1.923
5300	1.335		1.347		1.359		1.389	7.96×10^{-4}	1.397	7.58	1.400	5.86	1.887
5400	1.336		1.348		1.361		1.391	5.95	1.398	6.26	1.401	5.33	1.852
5500	1.338	2.50×10^{-4}	1.350		1.362		1.392	5.37	1.399	5.66	1.403	4.93	1.818
5600	1.339	2.37	1.351	2.87×10^{-4}	1.364		1.393	4.86	1.400	4.99	1.404	4.52	1.786
5700	1.340	2.09	1.352	2.68	1.365	3.00×10^{-4}	1.394	4.24	1.401	4.44	1.404	4.02	1.754
5800	1.341	1.87	1.353	2.37	1.366	2.65	1.396	3.61	1.402	3.76	1.405	3.48	1.724
5900	1.342	1.71	1.355	2.16	1.367	2.37	1.397	3.14	1.403	3.21	1.406	2.99	1.695
6000	1.342	1.58	1.356	1.98	1.368	2.18	1.398	2.72	1.404	2.76	1.407	2.55	1.667
6100	1.343	1.50	1.357	1.85	1.369	2.01	1.398	2.34	1.404	2.32	1.408	2.14	1.639
6200	1.344	1.48	1.358	1.73	1.370	1.87	1.399	2.02	1.405	1.95	1.409	1.81	1.613
6300	1.345	1.49	1.358	1.69	1.371	1.76	1.400	1.76	1.406	1.67	1.410	1.52	1.587
6400	1.346	1.55	1.359	1.72	1.372	1.68	1.402	1.55	1.407	1.41	1.410	1.24	1.563
6500	1.346	1.69	1.360	1.80	1.373	1.74	1.403	1.38	1.408	1.22	1.411	9.88×10^{-5}	1.538
6600	1.346	1.87	1.360	1.94	1.373	1.82	1.403	1.25	1.409	1.09	1.412	7.85	1.515
6700	1.347	2.17	1.361	2.14	1.374	1.91	1.404	1.17	1.410	9.41×10^{-5}	1.413	6.21	1.493
6800	1.348	2.43	1.362	2.28	1.375	1.99	1.405	1.10	1.410	8.13	1.414	4.53	1.471
6900	1.348	2.54	1.363	2.19	1.376	1.83	1.406	1.02	1.411	6.95	1.415	3.40	1.449
7000	1.349	2.36	1.363	1.72	1.377	1.47	1.406	8.78×10^{-5}	1.411	5.62	1.416	2.54	1.429
7100	1.349	1.60	1.364	1.04	1.377	8.80×10^{-5}	1.407	6.16	1.412	3.80	1.416	1.98	1.408
7200	1.350	7.52×10^{-5}	1.364	6.61×10^{-5}	1.377	5.35	1.408	3.89	1.413	2.61	1.416	1.65	1.389
7300	1.351	4.88	1.365	4.41	1.378	3.80	1.409	2.59	1.413	2.01	1.417	1.38	1.370
7400	1.351	3.37	1.366	3.06	1.378	2.69	1.410	1.98	1.414	1.53	1.418	1.15	1.351
7500	1.351	2.24	1.366	2.10	1.379	1.97	1.410	1.59	1.415	1.36	1.419	9.44×10^{-6}	1.333
7600	1.352	1.66	1.367	1.60	1.380	1.54	1.411	1.27	1.416	1.12	1.420	7.85	1.316
7700	1.352	1.33	1.367	1.29	1.380	1.26	1.411	1.05	1.416	9.50×10^{-6}	1.420	6.67	1.299
7800	1.353	1.13	1.368	1.10	1.381	1.07	1.412	8.93×10^{-6}	1.416	8.06	1.421	5.61	1.282
7900	1.353	1.03	1.368	9.74×10^{-6}	1.382	9.48×10^{-6}	1.413	7.75	1.417	6.88	1.422	4.68	1.266
8000	1.354	1.00	1.368	9.23	1.382	8.85	1.413	6.94	1.418	6.00	1.422	3.95	1.250
8200	1.355	1.02	1.369	8.98	1.383	8.22	1.415	5.63	1.419	4.72	1.422	2.91	1.220
8400	1.355	9.95×10^{-6}	1.369	8.83	1.384	7.90	1.416	4.95	1.420	3.85	1.423	2.29	1.190
8600	1.356	8.41	1.371	8.02	1.384	7.25	1.416	4.05	1.422	3.01	1.423	1.94	1.163
8800	1.357	4.46	1.371	4.04	1.385	3.73	1.417	2.46	1.422	2.17	1.424	1.69	1.136
9000	1.357	1.92	1.372	1.85	1.386	1.87	1.418	1.84	1.423	1.77	1.425	1.51	1.111
9200	1.358	1.44	1.373	1.43	1.387	1.45	1.419	1.60	1.424	1.60	1.425	1.44	1.087
9400	1.358	1.30	1.373	1.29	1.387	1.30	1.420	1.50	1.425	1.52	1.426	1.40	1.064
9600	1.358	1.49	1.374	1.39	1.388	1.37	1.421	1.48	1.425	1.46	1.426	1.32	1.042
9800	1.358	2.01	1.375	1.75	1.389	1.62	1.421	1.52	1.426	1.37	1.427	1.11	1.020
10000	1.359	2.75	1.375	2.36	1.389	2.09	1.422	1.53	1.427	1.19	1.427	8.67×10^{-7}	1.000
10200	1.359	3.23	1.376	2.86	1.390	2.40	1.422	1.41	1.427	9.67×10^{-7}	1.427	6.20	0.980
10400	1.360	2.91	1.377	2.51	1.390	1.97	1.423	1.03	1.428	7.51	1.427	4.53	0.962
10600	1.360	1.39	1.377	1.24	1.391	9.38×10^{-7}	1.423	6.05×10^{-7}	1.428	4.97	1.427	3.27	0.943
10800	1.360	7.88×10^{-7}	1.377	6.90×10^{-7}	1.391	5.25	1.424	3.62	1.429	3.49	1.428	2.39	0.926
11000	1.361	5.20	1.377	4.98	1.391	3.53	1.424	2.84	1.429	2.73	1.428	1.97	0.909
11200	1.361	4.01	1.378	3.79	1.392	2.65	1.425	2.33	1.430	2.15	1.428	1.71	0.893
11400	1.361	3.21	1.378	2.92	1.392	2.24	1.425	2.02	1.430	1.70	1.429	1.52	0.877
11600	1.361	2.72	1.379	2.50	1.392	2.07	1.425	1.83	1.431	1.48	1.429	1.34	0.862
11800	1.361	2.44	1.379	2.27	1.392	1.87	1.426	1.58	1.432	1.29	1.430	1.17	0.847
12000	1.362	1.92	1.380	1.73	1.392	1.42	1.426	1.24	1.432	1.07	1.430	9.95×10^{-8}	0.833
12200	1.362	1.25	1.380	1.14	1.392	1.04	1.427	9.98×10^{-8}	1.432	8.94×10^{-8}	1.430	8.35	0.820
12400	1.362	1.17	1.380	1.01	1.392	9.18×10^{-8}	1.427	8.79	1.432	7.51	1.430	7.06	0.806
12600	1.362	1.24	1.380	1.07	1.393	9.28	1.427	8.46	1.433	6.57	1.430	5.87	0.794
12800	1.362	1.32	1.380	1.14	1.393	9.51	1.427	8.39	1.433	6.09	1.431	4.85	0.781
13000	1.362	1.43	1.381	1.21	1.393	9.92	1.427	8.20	1.434	4.90	1.431	3.92	0.769
13200	1.362	1.55	1.381	1.25	1.393	1.04×10^{-7}	1.427	7.84	1.434	3.92	1.431	3.13	0.758
13400	1.362	1.45	1.381	1.18	1.393	9.86×10^{-8}	1.427	6.83	1.434	3.09	1.431	2.26	0.746
13600	1.362	1.09	1.381	8.89×10^{-8}	1.393	7.02	1.427	4.80	1.435	2.34	1.431		0.735
13800	1.363	6.86×10^{-8}	1.381	5.94	1.394	4.61	1.427	3.58	1.435	1.73	1.432		0.725
14000	1.363	4.72	1.381	3.87	1.394	3.13	1.427	2.79	1.435	1.14	1.432		0.714
14250	1.363	3.02	1.382	2.46	1.394	2.07	1.428	2.07	1.436		1.432		0.702
18000	1.366		1.384		1.397		1.431		1.438		1.434		0.556
22250	1.369		1.387		1.402		1.432		1.442		1.438		0.449
24500	1.373		1.392		1.408		1.438		1.448		1.443		0.408
27800	1.383		1.407		1.421		1.452		1.463		1.459		0.360

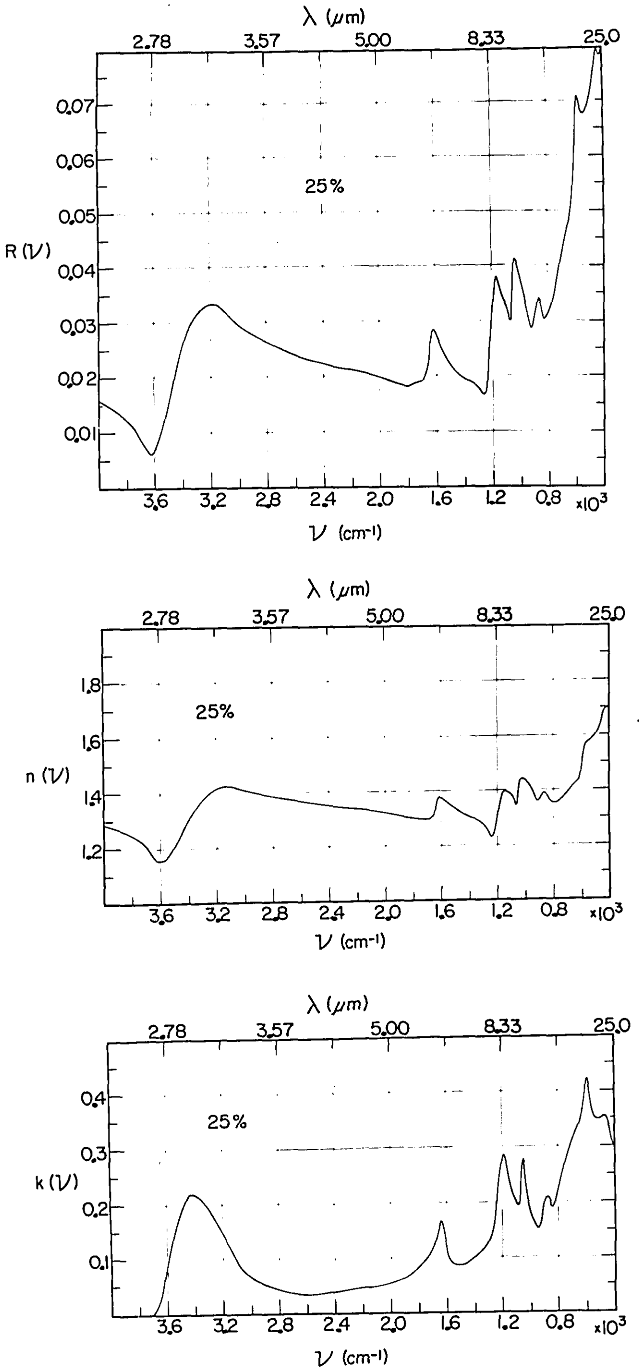

Fig. 5. Reflectivity, refractive index n, and absorption index k of a 25% H_2SO_4 solution in the intermediate infrared.

of the 4000–400 cm^{-1} range, the fractional uncertainty $\delta R/R$ was approximately ± 0.02, but was somewhat greater at the lowest frequencies. Plots of reflectance as a function of wavenumber are given in the upper panels of Figs. 5–10.

In obtaining n and k from measured reflectance R, we made use of the Kramers-Kronig phase-shift theorem,[8] which states: If the complex reflectivity $[R(\nu)]^{1/2} \exp [i\phi(\nu)]$ is known for all frequencies, the phase $\phi(\nu_0)$ at frequency ν_0 is given by the relation

$$\phi(\nu_0) = \frac{2\nu_0}{\pi} P\int_0^\infty \frac{\ln[R(\nu)]^{1/2}}{\nu_0^2 - \nu^2} d\nu, \tag{3}$$

where $[R(\nu)]^{1/2}$ and $\phi(\nu)$ must satisfy conditions that allow contour integration in the complex plane.

Equation (3) gives exact results, provided values of R are known for all frequencies. Since we have measured R for frequencies as high as 28000 cm^{-1} (Fig. 1) and wish to use Eq. (3) to give values of ϕ in the range of 4000–400 cm^{-1}, we introduce no appreciable

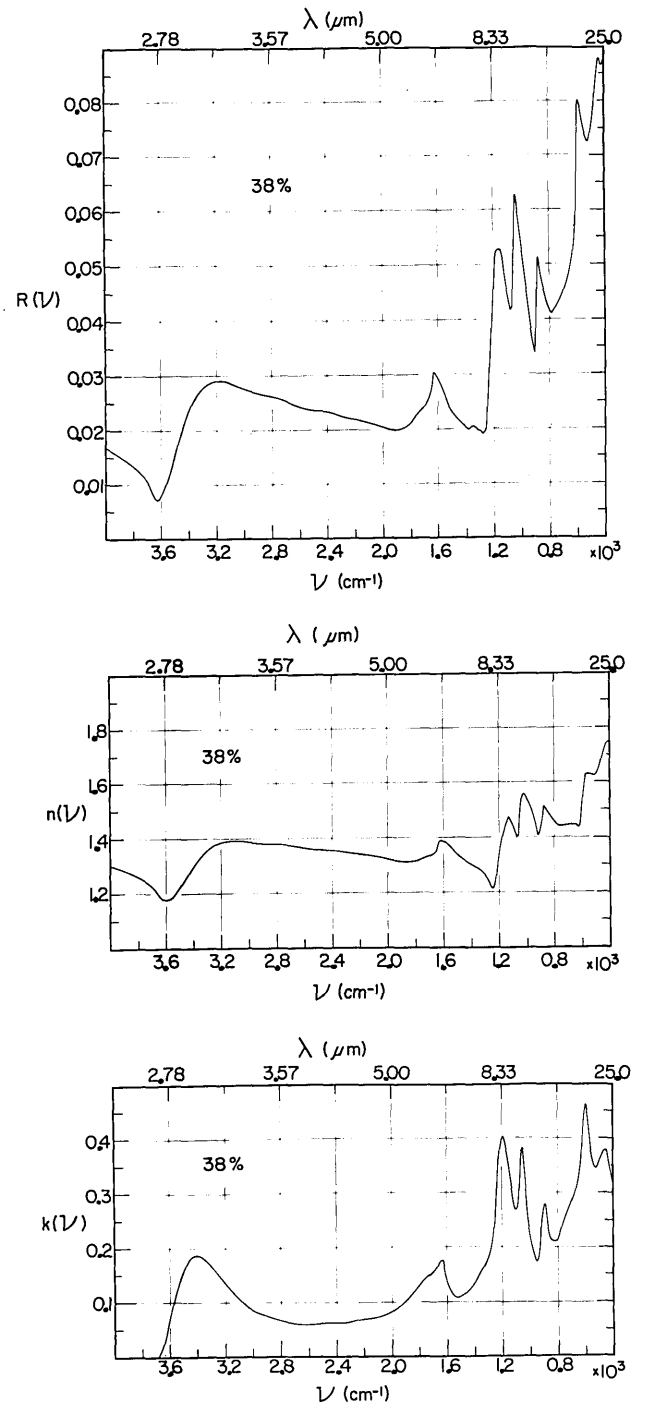

Fig. 6. Reflectivity, refractive index n, and absorption index k of a 38% H_2SO_4 solution in the intermediate infrared.

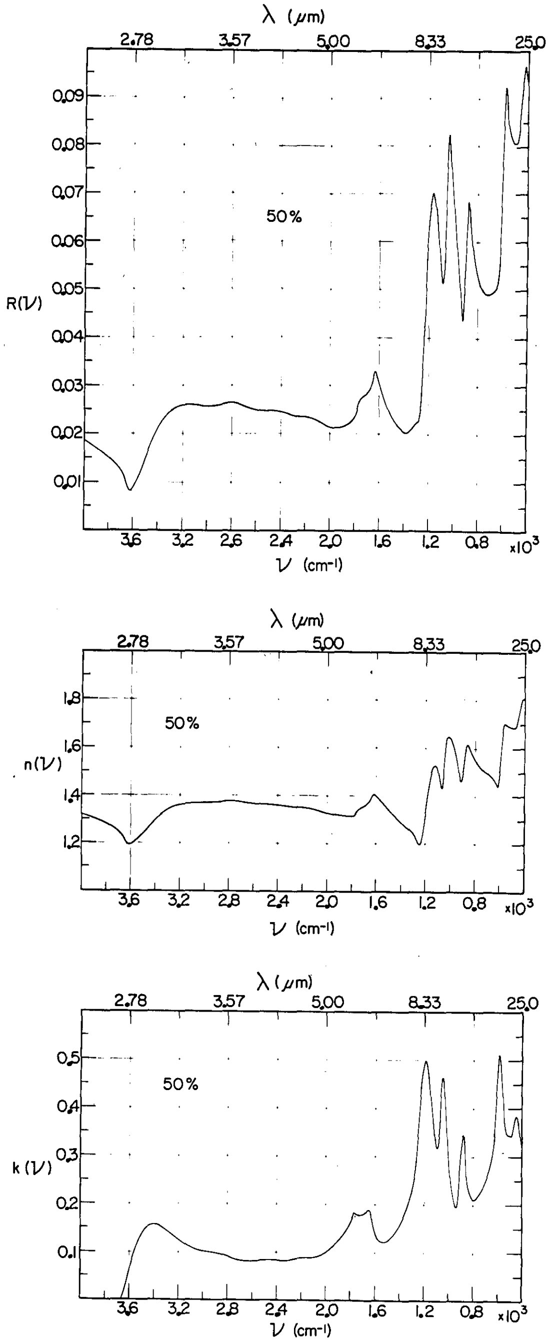

Fig. 7. Reflectivity, refractive index n, and absorption index k of a 50% H_2SO_4 solution in the intermediate infrared.

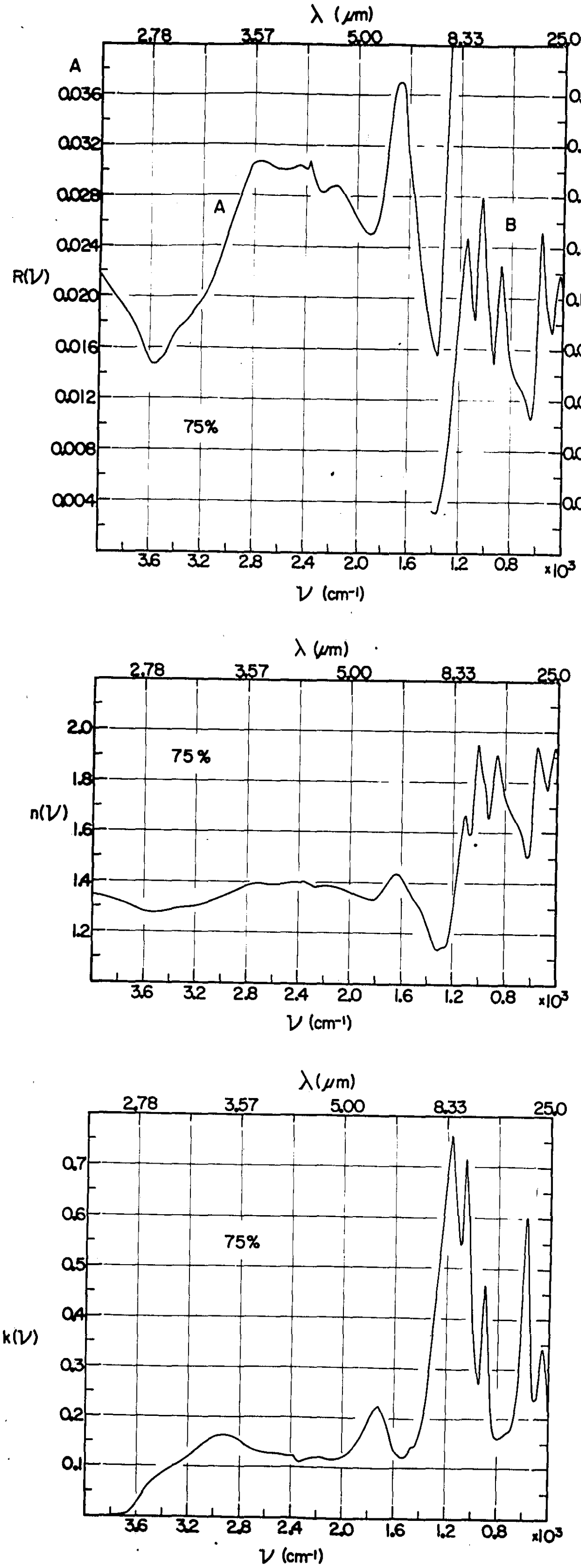

Fig. 8. Reflectivity, refractive index n, and absorption index k of a 75% H_2SO_4 solution in the intermediate infrared.

computational error in replacing infinity by 28000 cm^{-1} as the upper limit of the integral. This relative insensitivity to the upper limit is the result of the term $(\nu_0^2 - \nu^2)$ in the denominator of the integral, which becomes increasingly large as the upper limit is approached. Since we have no information regarding R for frequencies lower than 350 cm^{-1}, where our measurements ended, we are forced to make assumptions regarding reflectance in the far infrared. In evaluating Eq. (3), we have assumed that R in the remote infrared has a constant value equal to the measured value of R at 350 cm^{-1}. The influence of this value on $\phi(\nu_0)$ is greatest at low frequencies in the vicinity of 400 cm^{-1}, but in view of the term $(\nu_0^2 - \nu^2)$

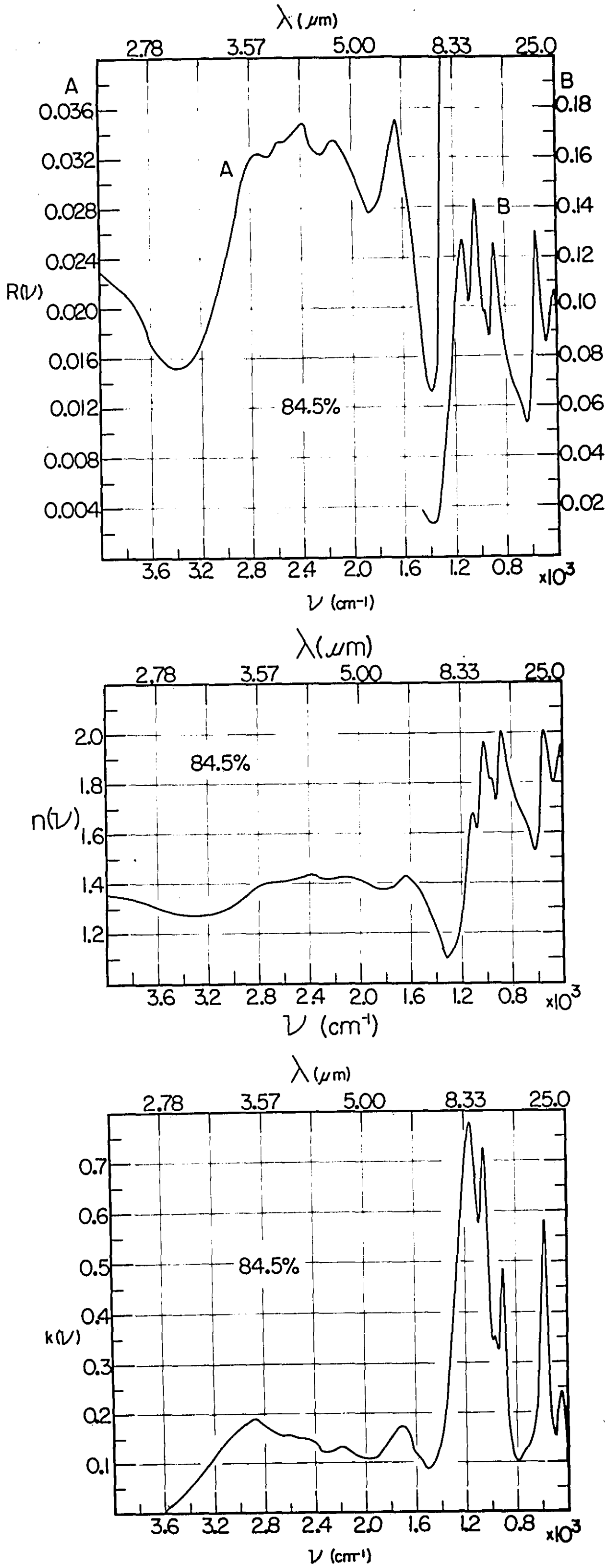

Fig. 9. Reflectivity, refractive index n, and absorption index k of an 84.5% H_2SO_4 solution in the intermediate infrared.

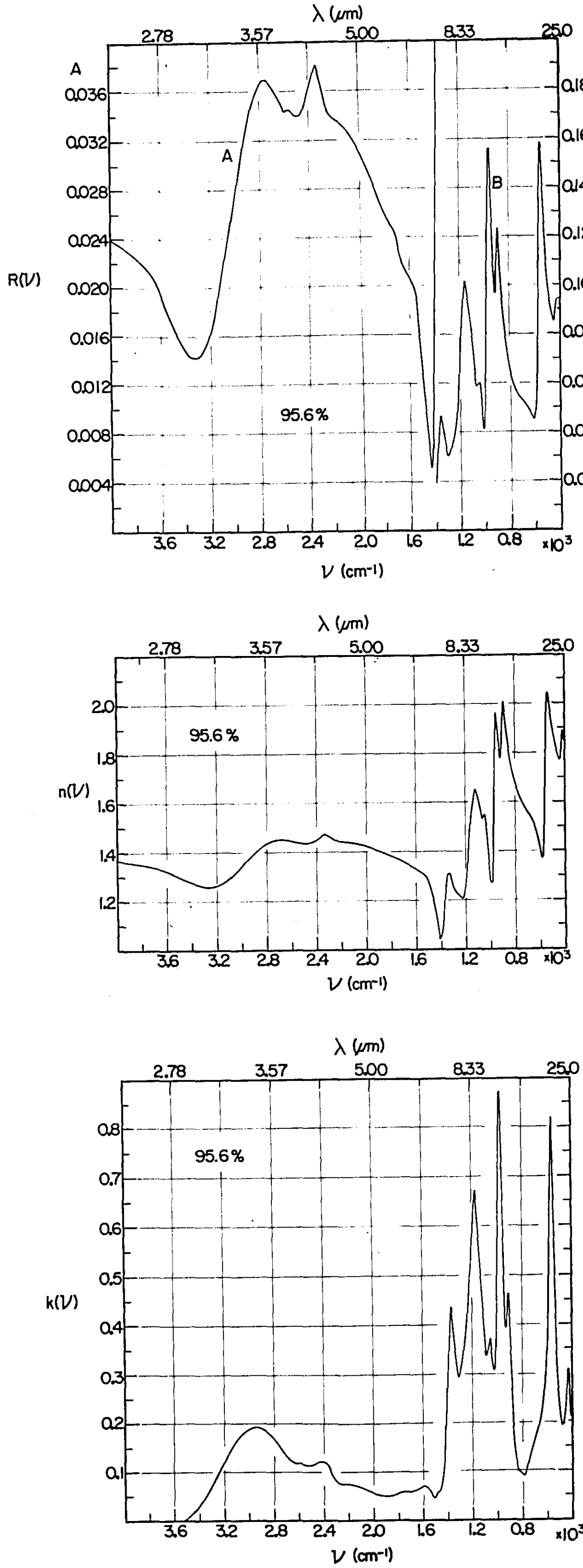

Fig. 10. Reflectivity, refractive index n, and absorption index k of a 95.6% H_2SO_4 solution in the infrared.

in the denominator of Eq. (3), it becomes progressively smaller as ν_0 increases.

Once the phase shift has been determined for a given frequency ν_0, the corresponding values of n and k at that frequency can be obtained from the relations

$$n = (1 - R)/(1 + R - 2R^{1/2}\cos\phi),$$
$$k = (-2R^{1/2}\sin\phi)/(1 + R - 2R^{1/2}\cos\phi). \quad (4)$$

The values of the optical constants n and k for the H_2SO_4 solutions are plotted as a function of wavenumber in the two lower panels of Figs. 5–10. The fractional uncertainty $\delta n/n$ is approximately ± 0.01 over most of the range but becomes larger at low frequencies because of increasing uncertainties in R and because of our extrapolation of R to frequencies lower than 350 cm^{-1}. The uncertainty δk is estimated as ± 0.03 over most of the range, but increases as 400 cm^{-1} is approached.

The spectral features of H_2SO_4 solutions in the intermediate infrared show marked changes with concentration. As a result of a beautiful study by Giguere and Savoie[14] covering the absorption spectrum in the range 5000–500 cm^{-1}, we can correlate most of the spectral features observed in the present study with the presence of H_2SO_4, HSO_4^-, SO_4^{--}, H_3O^+, H_2O, and various hydrates of H_2SO_4. Giguere and Savoie were primarily interested in an interpretation of their spectra in terms of various molecular and ionic species, and made no attempt to make quantitative measurements of intensity. Therefore, although our results are entirely compatible with theirs, we cannot make quantitative comparisons.

We summarize our present values of n and k in Table II, which lists n to four figures and k to three figures at various frequencies in the intermediate infrared. We emphasize once again that the uncertainties stated above should be considered by anyone making use of the tables in the interpretation of planetary or telluric spectra. The curves shown in Figs. 5–10 can be used to provide interpolated values of n and k at frequencies not listed in the table.

Discussion of Results

The values of n and k obtained in the present study can be compared with several other earlier studies. Our values for n covering the range from the near ultraviolet to the near infrared are in good agreement in the visible region with early measurements of n at discrete wavelengths in the visible region.[15] The early refractometer measurements of n, taken at several different temperatures by different investigators, have smaller uncertainties δn than the present values based upon spectral scans of reflectance. When Lorentz-Lorenz corrections are applied to earlier measurements in order to give values of n at 300 K, the resulting values fall within the range of uncertainty for our present values.

In Fig. 11 we give a comparison of our values of n and k for a 75% solution with those of Remsberg[2] in the region of the earth's atmospheric window in the 800–1200 cm^{-1} region. There is fair general agreement between major spectral features, as revealed in the two studies. Over most of the range, the Remsberg values fall within our stated range of uncertainties. Greater precision is usually claimed for ATR results than we claim for results based upon measurements of reflectance at a free liquid surface. It would therefore be desirable to extend the ATR measurements to the broad range of frequencies covered in our present survey.

In Figs. 12 and 13 we compare our results for the 25% solution with the recent results of Querry *et al.*,[16] based upon a Kramers-Kronig analysis of measurements of reflectance at nonnormal incidence in the spectral range 5000–500 cm^{-1}. There is good agreement between the studies, except in the low frequency region; lack of agreement in this region is not surprising, since the low frequency limits of the two studies were different and different extrapolations to zero frequency were made in the Kramers-Kronig analyses.

In this connection, we might note that better values of n and k could be obtained from our present reflectance measurements if reflectances could be extended to the submillimeter spectral region by the Fourier transform techniques developed by Chamberlain and his colleagues.[17,18] Use of reflectance values generated from values of n and k in Tables I and II, together with additional measurements between 400 cm^{-1} and 10 cm^{-1}, would virtually eliminate computational uncertainties in the evaluation of the integral in Eq. (3).

Because analyses of polarization data indicate that the particles in the Venus clouds are spherical, earlier workers have suggested that the particles consist of liquid droplets.[4] If this suggestion is correct, and if we assume that sulfuric acid solutions of all concentrations can be supercooled at 250 K, we can apply Lorentz-Lorenz corrections to convert our present values of n into equivalent values at 250 K, and we can compare our results with the values of n given by the recent analysis of Hansen and Hovenier[6]; in the Lorentz-Lorenz correction we used density values listed by Timmermans.[19] The results of such a comparison are summarized in Table III, in which we compare the Hansen-Hovenier values of n at three wavelengths with values of n for liquid samples of sulfuric acid solutions at 250 K. By recalling the uncertainties $\delta n \simeq \pm 0.015$ acceptable to Hansen and Hovenier, we can eliminate the sulfuric acid solutions of 50% or lower concentrations as having values of n below those acceptable. Within the limits of uncertainty, the 75, 84.5, and 95.6% solutions would be acceptable; however, for each of these solutions, our best values are higher than those of Hansen and Hovenier.

On the basis of a linear interpolation in values of n between the values for the 50 and 75% solutions, we have attempted to find the best match between our data and the results of the analysis of polarization data. A linear interpolation in this concentration range seems justified by early measurements of n in the visible region.[4] The best match is achieved for a concentration of 70.5%, which gives the values of n listed in the last column of Table III. Although this best-fit concentration is somewhat lower than Young's[4] early estimate of 75%, the two estimates are compatible within the limits of uncertainty.

Table II. Optical Constants of Sulfuric Acid in Intermediate Infrared

ν	25%		38%		50%		75%		84.5%		95.6%		λ
cm^{-1}	n	k	n	k	n	k	n	k	n	k	n	k	μm
400	1.700	0.303	1.749	0.327	1.806	0.319	1.930	0.200	1.938	0.099	1.896	0.212	25.000
410	1.696	0.305	1.744	0.328	1.808	0.328	1.939	0.226	1.954	0.144	1.880	0.245	24.390
430	1.692	0.329	1.736	0.356	1.783	0.371	1.918	0.300	1.905	0.219	1.822	0.274	23.256
440	1.676	0.343	1.719	0.372	1.758	0.380	1.881	0.320	1.874	0.231	1.781	0.248	22.727
450	1.657	0.351	1.696	0.378	1.734	0.384	1.848	0.329	1.846	0.229	1.785	0.218	22.222
470	1.627	0.354	1.658	0.374	1.689	0.361	1.781	0.290	1.807	0.199	1.826	0.193	21.277
480	1.615	0.353	1.645	0.368	1.690	0.350	1.782	0.257	1.804	0.169	1.848	0.194	20.833
490	1.605	0.351	1.635	0.363	1.690	0.345	1.804	0.240	1.833	0.145	1.874	0.197	20.408
500	1.596	0.349	1.627	0.357	1.690	0.344	1.823	0.235	1.873	0.146	1.913	0.209	20.000
510	1.590	0.349	1.622	0.349	1.690	0.344	1.842	0.238	1.903	0.161	1.961	0.241	19.608
530	1.580	0.352	1.627	0.348	1.692	0.353	1.892	0.261	1.981	0.216	2.057	0.405	18.868
540	1.576	0.355	1.628	0.354	1.694	0.360	1.926	0.299	2.011	0.291	2.045	0.569	18.519
550	1.572	0.360	1.629	0.364	1.700	0.375	1.946	0.362	2.011	0.391	1.912	0.740	18.182
560	1.569	0.368	1.629	0.379	1.703	0.402	1.939	0.457	1.955	0.520	1.680	0.802	17.857
570	1.564	0.383	1.625	0.404	1.693	0.443	1.869	0.554	1.800	0.575	1.477	0.699	17.544
580	1.550	0.412	1.603	0.443	1.653	0.496	1.741	0.594	1.671	0.549	1.389	0.540	17.241
590	1.509	0.422	1.551	0.460	1.576	0.509	1.621	0.564	1.584	0.468	1.382	0.415	16.949
600	1.473	0.415	1.498	0.448	1.506	0.479	1.542	0.479	1.552	0.400	1.410	0.340	16.667
620	1.433	0.374	1.438	0.381	1.441	0.379	1.512	0.352	1.530	0.290	1.466	0.253	16.129
630	1.427	0.358	1.437	0.350	1.450	0.338	1.512	0.299	1.538	0.244	1.488	0.232	15.873
650	1.420	0.340	1.445	0.322	1.472	0.299	1.551	0.221	1.578	0.175	1.520	0.203	15.385
670	1.407	0.329	1.444	0.304	1.483	0.277	1.596	0.191	1.617	0.151	1.543	0.183	14.925
680	1.400	0.322	1.443	0.295	1.488	0.268	1.613	0.183	1.632	0.144	1.552	0.176	14.706
700	1.388	0.309	1.441	0.280	1.496	0.254	1.643	0.173	1.657	0.134	1.567	0.160	14.286
720	1.377	0.294	1.440	0.266	1.503	0.242	1.663	0.171	1.677	0.125	1.584	0.143	13.889
740	1.367	0.279	1.440	0.253	1.511	0.230	1.681	0.165	1.698	0.116	1.604	0.126	13.514
760	1.358	0.262	1.440	0.240	1.520	0.221	1.701	0.160	1.722	0.108	1.628	0.110	13.158
780	1.353	0.242	1.443	0.226	1.532	0.213	1.726	0.157	1.751	0.100	1.663	0.090	12.821
790	1.353	0.233	1.447	0.218	1.541	0.210	1.741	0.157	1.771	0.099	1.693	0.090	12.658
800	1.354	0.224	1.455	0.211	1.549	0.210	1.757	0.158	1.793	0.100	1.710	0.094	12.500
820	1.357	0.206	1.471	0.209	1.568	0.215	1.796	0.168	1.839	0.112	1.751	0.096	12.195
840	1.373	0.191	1.483	0.212	1.588	0.227	1.844	0.194	1.896	0.130	1.812	0.107	11.905
850	1.382	0.190	1.491	0.216	1.599	0.238	1.869	0.216	1.934	0.158	1.848	0.121	11.765
870	1.392	0.205	1.512	0.240	1.617	0.303	1.916	0.313	1.993	0.247	1.940	0.181	11.494
874	1.385	0.208	1.515	0.259	1.607	0.338	1.911	0.341	1.998	0.277	1.956	0.206	11.442
880	1.381	0.209	1.491	0.275	1.579	0.345	1.904	0.386	2.005	0.321	1.978	0.243	11.364
890	1.372	0.207	1.461	0.277	1.519	0.338	1.842	0.464	1.984	0.416	2.007	0.356	11.236
900	1.365	0.200	1.436	0.269	1.484	0.311	1.739	0.463	1.884	0.483	1.937	0.458	11.111
910	1.360	0.188	1.416	0.247	1.471	0.279	1.676	0.410	1.789	0.466	1.841	0.460	10.989
920	1.360	0.173	1.407	0.207	1.463	0.228	1.663	0.351	1.735	0.402	1.808	0.407	10.870
930	1.368	0.160	1.431	0.184	1.502	0.200	1.678	0.301	1.742	0.348	1.870	0.391	10.753
940	1.382	0.152	1.454	0.173	1.535	0.192	1.717	0.275	1.775	0.323	1.953	0.468	10.638
950	1.396	0.151	1.475	0.172	1.563	0.199	1.756	0.271	1.807	0.328	1.967	0.627	10.526
960	1.407	0.154	1.495	0.176	1.582	0.210	1.788	0.277	1.820	0.346	1.856	0.795	10.417
963	1.412	0.157	1.501	0.181	1.587	0.215	1.807	0.282	1.820	0.349	1.789	0.833	10.384
970	1.417	0.158	1.510	0.186	1.597	0.222	1.822	0.292	1.818	0.347	1.634	0.869	10.309
980	1.425	0.165	1.523	0.197	1.613	0.235	1.849	0.311	1.839	0.341	1.415	0.809	10.204
990	1.432	0.173	1.535	0.212	1.631	0.255	1.882	0.338	1.877	0.353	1.301	0.624	10.101
1010	1.441	0.195	1.549	0.247	1.650	0.314	1.947	0.453	1.954	0.443	1.372	0.350	9.901
1020	1.442	0.209	1.556	0.272	1.649	0.349	1.944	0.538	1.968	0.528	1.457	0.311	9.804
1030	1.438	0.226	1.557	0.314	1.644	0.402	1.907	0.637	1.937	0.630	1.527	0.326	9.709
1040	1.431	0.246	1.525	0.364	1.594	0.463	1.807	0.708	1.848	0.707	1.548	0.352	9.615
1050	1.398	0.273	1.460	0.376	1.509	0.462	1.702	0.711	1.749	0.724	1.548	0.373	9.524
1060	1.350	0.245	1.407	0.339	1.456	0.428	1.624	0.668	1.666	0.693	1.537	0.366	9.434
1070	1.346	0.213	1.396	0.297	1.433	0.370	1.589	0.612	1.625	0.639	1.548	0.347	9.346
1080	1.362	0.194	1.419	0.266	1.450	0.337	1.590	0.560	1.623	0.594	1.578	0.342	9.259
1090	1.377	0.193	1.434	0.265	1.471	0.314	1.626	0.540	1.647	0.574	1.617	0.360	9.174
1100	1.383	0.197	1.442	0.267	1.502	0.318	1.655	0.556	1.682	0.603	1.639	0.391	9.091
1110	1.387	0.201	1.452	0.269	1.523	0.335	1.669	0.590	1.682	0.634	1.654	0.439	9.009
1120	1.389	0.206	1.464	0.280	1.529	0.360	1.666	0.634	1.670	0.686	1.645	0.481	8.929
1130	1.391	0.211	1.473	0.302	1.529	0.384	1.643	0.681	1.633	0.731	1.632	0.524	8.850
1150	1.395	0.229	1.451	0.344	1.507	0.436	1.545	0.755	1.515	0.777	1.572	0.615	8.696
1160	1.393	0.246	1.435	0.360	1.483	0.465	1.479	0.761	1.456	0.773	1.516	0.651	8.621
1170	1.382	0.268	1.417	0.376	1.448	0.485	1.421	0.758	1.403	0.764	1.447	0.669	8.547
1190	1.329	0.285	1.353	0.400	1.369	0.498	1.320	0.719	1.308	0.726	1.300	0.643	8.403
1210	1.277	0.270	1.283	0.381	1.280	0.473	1.241	0.663	1.230	0.666	1.230	0.532	8.264
1230	1.238	0.228	1.222	0.322	1.218	0.409	1.179	0.593	1.179	0.590	1.217	0.453	8.130
1240	1.230	0.199	1.212	0.285	1.203	0.370	1.161	0.547	1.166	0.557	1.219	0.427	8.065
1250	1.233	0.173	1.214	0.252	1.197	0.329	1.151	0.513	1.153	0.527	1.218	0.400	8.000
1270	1.254	0.143	1.236	0.206	1.212	0.268	1.145	0.445	1.132	0.471	1.225	0.358	7.874
1290	1.271	0.127	1.258	0.184	1.239	0.239	1.144	0.397	1.116	0.412	1.244	0.321	7.752
1310	1.284	0.121	1.269	0.172	1.251	0.222	1.136	0.351	1.102	0.351	1.276	0.308	7.634
1320	1.288	0.119	1.275	0.166	1.255	0.214	1.133	0.323	1.100	0.318	1.292	0.313	7.576
1340	1.293	0.115	1.284	0.157	1.263	0.197	1.142	0.262	1.116	0.242	1.314	0.362	7.463
1360	1.297	0.109	1.290	0.152	1.272	0.182	1.173	0.211	1.156	0.201	1.245	0.431	7.353
1370	1.300	0.107	1.290	0.146	1.275	0.175	1.192	0.195	1.171	0.187	1.180	0.437	7.299

ν	25%		38%		50%		75%		84.5%		95.6%		λ
cm^{-1}	n	k	n	k	n	k	n	k	n	k	n	k	μm
1390	1.304	0.102	1.297	0.135	1.285	0.161	1.222	0.173	1.197	0.161	1.057	0.334	7.194
1410	1.309	0.097	1.305	0.127	1.296	0.150	1.249	0.158	1.219	0.138	1.024	0.226	7.092
1430	1.313	0.092	1.313	0.121	1.307	0.143	1.272	0.143	1.246	0.116	1.092	0.100	6.993
1450	1.319	0.089	1.322	0.117	1.315	0.136	1.297	0.143	1.273	0.102	1.159	0.067	6.897
1470	1.325	0.086	1.327	0.112	1.325	0.130	1.308	0.137	1.299	0.094	1.209	0.058	6.803
1490	1.332	0.084	1.335	0.108	1.335	0.125	1.323	0.130	1.323	0.088	1.237	0.052	6.711
1500	1.335	0.083	1.339	0.107	1.340	0.122	1.331	0.126	1.335	0.087	1.252	0.047	6.667
1510	1.339	0.083	1.344	0.106	1.346	0.121	1.340	0.122	1.347	0.087	1.270	0.045	6.623
1520	1.342	0.083	1.349	0.105	1.352	0.120	1.351	0.121	1.360	0.088	1.285	0.048	6.579
1530	1.346	0.083	1.354	0.104	1.357	0.120	1.361	0.122	1.371	0.093	1.297	0.052	6.536
1540	1.351	0.085	1.360	0.105	1.363	0.120	1.368	0.123	1.378	0.098	1.305	0.056	6.494
1560	1.359	0.088	1.371	0.111	1.375	0.122	1.384	0.125	1.389	0.105	1.318	0.065	6.410
1580	1.368	0.096	1.380	0.120	1.386	0.128	1.399	0.130	1.400	0.111	1.322	0.070	6.329
1600	1.378	0.112	1.385	0.135	1.398	0.138	1.413	0.138	1.410	0.116	1.326	0.069	6.250
1610	1.379	0.125	1.387	0.143	1.403	0.148	1.422	0.144	1.416	0.120	1.329	0.069	6.211
1620	1.374	0.139	1.386	0.154	1.406	0.159	1.428	0.152	1.422	0.126	1.331	0.068	6.173
1630	1.365	0.156	1.381	0.170	1.402	0.172	1.434	0.164	1.427	0.133	1.333	0.067	6.135
1640	1.344	0.165	1.361	0.174	1.395	0.185	1.433	0.175	1.430	0.143	1.336	0.065	6.098
1650	1.321	0.159	1.349	0.170	1.379	0.187	1.430	0.184	1.429	0.153	1.339	0.064	6.061
1660	1.310	0.148	1.343	0.165	1.371	0.185	1.427	0.191	1.425	0.161	1.341	0.062	6.024
1680	1.299	0.130	1.335	0.157	1.361	0.181	1.420	0.203	1.413	0.169	1.347	0.057	5.952
1700	1.296	0.116	1.330	0.151	1.356	0.177	1.410	0.215	1.404	0.173	1.357	0.054	5.882
1720	1.298	0.105	1.327	0.147	1.352	0.176	1.392	0.225	1.394	0.173	1.365	0.057	5.814
1740	1.300	0.099	1.323	0.143	1.347	0.177	1.371	0.220	1.385	0.169	1.369	0.058	5.747
1760	1.300	0.094	1.317	0.139	1.340	0.181	1.361	0.212	1.377	0.162	1.371	0.058	5.682
1770	1.299	0.091	1.315	0.136	1.330	0.182	1.356	0.209	1.375	0.158	1.373	0.057	5.650
1780	1.299	0.088	1.314	0.133	1.319	0.173	1.350	0.206	1.374	0.154	1.375	0.056	5.618
1800	1.299	0.082	1.311	0.126	1.316	0.160	1.341	0.194	1.373	0.146	1.379	0.055	5.556
1820	1.301	0.076	1.310	0.119	1.316	0.151	1.337	0.182	1.373	0.140	1.384	0.053	5.495
1840	1.303	0.071	1.309	0.114	1.314	0.143	1.336	0.171	1.374	0.134	1.387	0.052	5.435
1860	1.306	0.068	1.310	0.107	1.315	0.136	1.336	0.160	1.375	0.127	1.393	0.051	5.376
1880	1.309	0.064	1.310	0.103	1.315	0.130	1.339	0.151	1.378	0.119	1.397	0.051	5.319
1900	1.311	0.061	1.312	0.097	1.316	0.123	1.342	0.144	1.385	0.113	1.403	0.050	5.263
1930	1.315	0.058	1.314	0.090	1.318	0.116	1.347	0.135	1.393	0.110	1.409	0.052	5.181
1960	1.317	0.055	1.318	0.085	1.321	0.108	1.353	0.128	1.401	0.108	1.416	0.053	5.102
2020	1.324	0.049	1.324	0.076	1.329	0.096	1.366	0.118	1.414	0.110	1.426	0.058	4.950
2080	1.330	0.046	1.330	0.071	1.338	0.089	1.379	0.116	1.423	0.116	1.434	0.064	4.808
2120	1.333	0.044	1.335	0.068	1.343	0.087	1.384	0.117	1.426	0.122	1.438	0.069	4.717
2180	1.337	0.043	1.340	0.065	1.348	0.086	1.386	0.121	1.422	0.131	1.441	0.074	4.587
2240	1.340	0.042	1.343	0.063	1.350	0.085	1.384	0.119	1.416	0.127	1.446	0.075	4.464
2290	1.341	0.040	1.345	0.060	1.352	0.081	1.386	0.113	1.419	0.122	1.457	0.077	4.367
2330	1.343	0.036	1.349	0.057	1.357	0.079	1.395	0.109	1.425	0.122	1.470	0.092	4.292
2340	1.344	0.036	1.350	0.057	1.357	0.079	1.397	0.110	1.428	0.122	1.472	0.099	4.274
2370	1.347	0.035	1.354	0.058	1.359	0.080	1.405	0.117	1.436	0.131	1.461	0.116	4.219
2410	1.350	0.034	1.356	0.059	1.361	0.080	1.399	0.121	1.430	0.142	1.446	0.120	4.149
2450	1.353	0.033	1.356	0.058	1.362	0.080	1.400	0.124	1.425	0.146	1.438	0.118	4.082
2500	1.355	0.032	1.358	0.056	1.363	0.080	1.398	0.126	1.418	0.149	1.435	0.114	4.000
2530	1.357	0.030	1.359	0.056	1.363	0.080	1.396	0.127	1.416	0.150	1.436	0.113	3.953
2560	1.361	0.030	1.361	0.054	1.364	0.078	1.395	0.127	1.414	0.152	1.438	0.115	3.906
2590	1.364	0.029	1.363	0.053	1.365	0.078	1.395	0.127	1.412	0.156	1.437	0.118	3.861
2600	1.364	0.028	1.364	0.053	1.365	0.077	1.395	0.127	1.410	0.157	1.437	0.117	3.846
2620	1.367	0.029	1.366	0.052	1.366	0.077	1.396	0.128	1.406	0.157	1.438	0.116	3.817
2660	1.372	0.029	1.370	0.052	1.369	0.076	1.396	0.130	1.403	0.156	1.445	0.122	3.759
2710	1.377	0.030	1.375	0.054	1.374	0.077	1.397	0.136	1.402	0.159	1.448	0.137	3.690
2760	1.384	0.031	1.379	0.056	1.378	0.081	1.394	0.143	1.399	0.168	1.444	0.155	3.623
2810	1.391	0.034	1.383	0.059	1.379	0.086	1.388	0.153	1.388	0.178	1.431	0.173	3.559
2880	1.400	0.040	1.389	0.064	1.377	0.092	1.370	0.161	1.361	0.189	1.403	0.192	3.472
2930	1.408	0.047	1.393	0.070	1.375	0.095	1.357	0.159	1.341	0.181	1.377	0.197	3.413
2990	1.418	0.058	1.397	0.078	1.373	0.099	1.341	0.159	1.321	0.171	1.347	0.195	3.344
3050	1.428	0.075	1.401	0.090	1.371	0.102	1.325	0.150	1.306	0.159	1.315	0.182	3.279
3150	1.431	0.118	1.400	0.117	1.369	0.113	1.306	0.131	1.283	0.131	1.274	0.143	3.175
3250	1.408	0.166	1.380	0.149	1.357	0.130	1.296	0.109	1.273	0.098	1.260	0.092	3.077
3310	1.380	0.193	1.359	0.165	1.343	0.141	1.294	0.099	1.272	0.079	1.263	0.064	3.021
3350	1.354	0.207	1.342	0.175	1.330	0.148	1.292	0.093	1.273	0.067	1.267	0.048	2.985
3400	1.313	0.218	1.312	0.184	1.308	0.154	1.288	0.086	1.276	0.053	1.276	0.030	2.941
3430	1.285	0.219	1.290	0.185	1.291	0.153	1.284	0.082	1.277	0.045	1.283	0.022	2.915
3470	1.243	0.206	1.256	0.176	1.267	0.147	1.277	0.073	1.282	0.034	1.291	0.012	2.882
3520	1.204	0.174	1.222	0.150	1.238	0.125	1.273	0.056	1.289	0.022	1.303		2.841
3530	1.198	0.166	1.216	0.144	1.233	0.119	1.272	0.052	1.290	0.019	1.305		2.833
3610	1.170	0.089	1.191	0.077	1.215	0.062	1.277	0.023	1.304		1.327		2.770
3620	1.171	0.079	1.190	0.068	1.216	0.054	1.279	0.019	1.307		1.329		2.762
3670	1.183	0.031	1.207	0.025	1.231	0.022	1.293	0.006	1.320		1.339		2.725
3720	1.216		1.234		1.252		1.308		1.330		1.345		2.688
3800	1.250		1.266		1.282		1.320		1.341		1.353		2.632
3900	1.271		1.284		1.299		1.332		1.348		1.360		2.564
4000	1.286		1.300		1.311		1.344		1.358		1.368		2.500

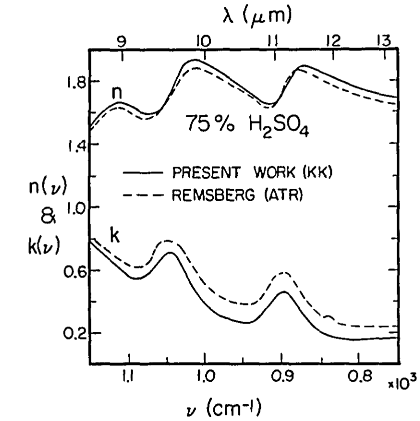

Fig. 11. Comparison of present results *(solid curves)* with those of Remsberg *(dashed curves)* for a 75% solution.

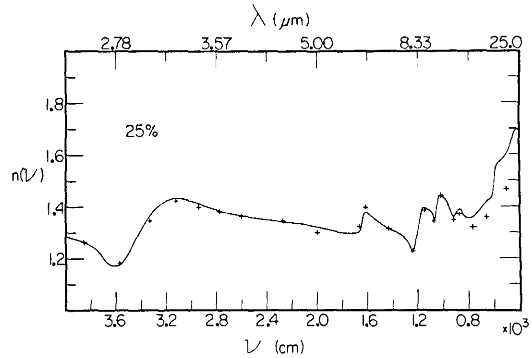

Fig. 12. Comparison of present results for the refractive index n *(solid curve)* with those of Querry *et al.* *(crosses)* for a 25% solution.

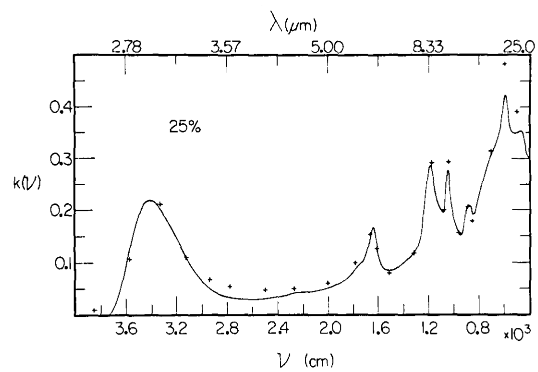

Fig. 13. Comparison of present results for the absorption index k *(solid curve)* with those of Querry *et al.* *(crosses)* for a 25% solution.

The assumption of supercooling solutions to 250 K is highly questionable. Figure 14 gives the phase-equilibrium curve between solutions of the indicated composition and the indicated crystalline solids. If we start with solutions at 300 K and assume that cooling occurs under equilibrium conditions, we should expect that cooling at 250 K would have the following results: (1) crystalline H_2SO_4 would form if solutions with initial concentrations greater than 95% H_2SO_4 were cooled, and less concentrated solutions would result; (2) for solutions with initial concentrations in the range between 75% and 93%, the crystalline monohydrate $H_2SO_4 \cdot H_2O$ would be formed in equilibrium with solutions of altered concentrations; (3) in the initial concentration range between 26% and 75%, all solutions would remain liquid without any change in concentration; and (4) for initial concentrations below 26%, ice in equilibrium with solutions of altered concentration would be formed. Under equilibrium conditions, only solutions in the ranges 26–75% and 93–95% H_2SO_4 would remain liquid as the temperature is reduced from 300 K to 250 K.

If the particles in the Venus clouds are actually liquid sulfuric acid droplets, it is difficult to understand why energetically favored agglomeration of the droplets does not occur; the sharply peaked distribution, reported by Hansen and Hovenier, indicates that agglomeration is inhibited. Another interesting question involves the internal pressure $P = P_0 + 2\sigma/r$ of liquid droplets; use of Timmerman's[20] values of surface tension σ gives a total internal pressure P of a liquid droplet as approximately 1 atm for spherical

Table III. Comparison of *n* Values in the Optical Region

Wavelength (nm)	Venus clouds[a]	Sulfuric Acid Solutions at 250 K 50%	75%	84.5%[b]	95.6%[b]	70.5%[c]
990	1.43	1.40	1.44	1.44	1.44	1.43
548	1.44	1.41	1.445	1.445	1.45	1.44
364	1.46	1.43	1.47	1.48	1.47	1.46

[a] Hansen and Hovenier.
[b] Supercooling required.
[c] Interpolated values.

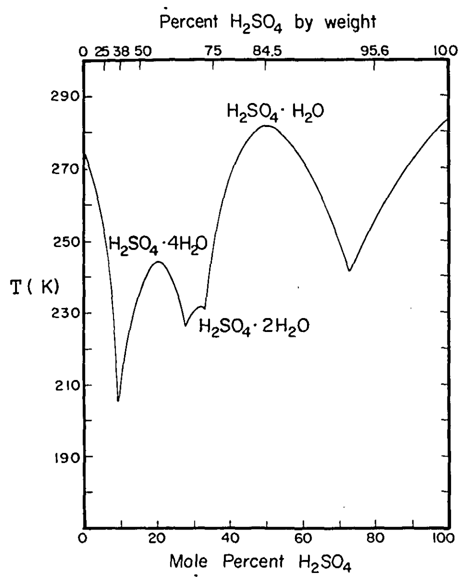

Fig. 14. The melting-point curve for H_2SO_4 solutions at a pressure of 1 atm.

particles in a region where the external pressure P_0 is only 50 mbars. The possibility of particles with solid nuclei cannot be entirely ignored; if the solid nuclei consisted of crystalline hydrates of H_2SO_4, the difference in n between the solid nucleus and the surrounding liquid might be so small as to escape detection in the analysis of scattering and polarization. The presence of solid nuclei might also serve to inhibit agglomeration.

Spectra of Venus in the intermediate infrared, as observed from ground-based observatories, has been limited to regions observable through the earth's atmospheric windows. Young[21] has recently compared observed Venus spectra with Remsberg's laboratory data[2] in the 800–1200 cm^{-1} window; Young reports similarity between the observed spectra and the spectra predicted on the basis of a model involving liquid droplets of sulfuric acid with a concentration of 75%. Pollack[22] and his associates have recently compared Venus spectra in the 3-μm region, as observed from high altitude jet aircraft, with predictions based upon preliminary values of our optical constants; concentrations of 75% and 90% seem to be compatible with the observed spectrum.

Improved intermediate infrared spectra of Venus could provide definitive evidence regarding the possibility of sulfuric acid as a major component of the planet's cloud cover. We hope that our present values of optical constants will be useful in the interpretation of future Venus spectra in both the solar-reflectance and thermal-emission regions. If future observations show that sulfuric acid is indeed the dominant component and the observations can further narrow the ranges of possible H_2SO_4 concentrations, further laboratory studies of H_2SO_4 solutions within these ranges should be conducted at reduced temperatures.

On the basis of our present work, along with the assumption that the Venus clouds do consist of spherical liquid droplets of sulfuric acid at 250 K, our best estimate is that the H_2SO_4 solution has a concentration of 70.5%. However, some of the difficulties outlined above must be resolved before our conclusion can be seriously regarded. Meanwhile, we also express the hope that our present work may prove useful to investigations of the earth's major stratospheric aerosol.

We gratefully acknowledge helpful discussions with J. B. Pollack and J. W. Hovenier. This work was supported in part by the National Aeronautics and Space Administration.

References

1. J. M. Rosen, J. Appl. Meterol. **10**, 1044 (1971).
2. E. E. Remsberg, J. Geophys. Res. **78**, 1401 (1973).
3. J. Neumann, J. Atmos. Sci. **30**, 95 (1973).
4. A. T. Young, Icarus **18**, 564 (1973).
5. G. T. Sill, Commun. Lun. Plan. Lab. **9**, 191 (1972).
6. J. E. Hansen and J. W. Hovenier, J. Atmos. Sci. **31**, 1137 (1974).
7. A. N. Rusk, D. Williams, and M. R. Querry, J. Opt. Soc. Am. **59**, 1299 (1971).
8. G. M. Hale, M. R. Querry, A. N. Rusk, and D. Williams, J. Opt. Soc. Am. **62**, 1103 (1972).
9. C. W. Robertson and D. Williams. J. Opt. Soc. Am. **61**, 1316 (1971).
10. J. W. Schaaf and D. Williams, J. Opt. Soc. Am. **63**, 726 (1973).
11. C. W. Robertson, B. Curnutte, and D. Williams, Mol. Phys. **26**, 183 (1973).
12. K. F. Palmer and D. Williams, J. Opt. Soc. Am. **64**, 1107 (1974).
13. E. K. Plyler and E. S. Barr, J. Chem. Phys. **2**, 306 (1936).
14. P. A. Giguere and R. Savoie, Can. J. Chem. **38**, 2467 (1960).
15. J. Timmermans, *The Physico-Chemical Constants of Binary Systems in Concentrated Solutions* (Interscience, New York, 1960) Vol. 4, pp. 569–571.
16. M. R. Querry, R. C. Waring, W. E. Holland, L. M. Earls, M. D. Herrman, W. P. Nijm, and G. M. Hale, J. Opt. Soc. Am. **64**, 39 (1974).
17. M. Davies, G. W. F. Pardoe, J. Chamberlain, and H. A. Gebbie, Trans. Faraday Soc. **66**, 273 (1970).
18. M. S. Zafur, J. B. Hasted, and J. Chamberlain, Nature: Phys. Sci. **243**, 106 (1973).
19. Ref. 15, pp. 561–562.
20. Ref. 15, pp. 568–569.
21. A. T. Young, Science **183**, 407 (1974).
22. J. B. Pollack (private communication).

Arctic Bulletin

Arctic Bulletin, Vol. 1, No. 4, published by NSF for the Interagency Arctic Research Coordinating Committee, contains articles on the Arctic Ice Dynamics Joint Experiment, the Beaufort Sea Symposium, the Environmental Data Service's arctic information system, and other subjects. Single copies or subscriptions to the quarterly magazine are free from the Office of Polar Programs, NSF, Wash., D.C. 20550.